Research Paper
International Journal of Aerospace System Engineering
Vol.2, No.1, pp.53-57 (2015)
ISSN 2383-4986

Aerodynamic Design of a Novel Low-Reynolds-Number Airfoil for Near Space Propellers

Shunlei Zhang[1,†], Xudong Yang[1], Bifeng Song[1] and Wenping Song[1]
[1] *School of Aeronautics, Northwestern Polytechnical University, Xi'an, China*

Abstract : For improving the efficiency of near space propellers working over 20km, performances of their streamwise sections, i.e. low-Reynolds-number airfoils which work at 10^4-10^5 Reynolds numbers, are significant. Based on the low-Reynolds-number CFD technology, this paper designs a novel low-Reynolds-number airfoil. Unsteady characteristics of the laminar separation bubble on the novel airfoil and a typical conventional airfoil are studied numerically, and the Reynolds number effect is investigated. Results show that at 10^4-10^5 Reynolds numbers, unsteady aerodynamic characteristics of the novel airfoil are severely weakened and its lift-to-drag ratio can increase about 100%.

Key Words : Near space, Low Reynolds number, Airfoil, Laminar separation bubble

1. Introduction

The propulsion system using propellers is most effective for near spacecrafts working over 20km. The efficiency of near space propellers affects near spacecrafts' weight and energy configuration, and improving performances of their streamwise sections (i.e. airfoils) becomes extremely important. However, the atmospheric density on the ground is fourteen times of that at 20km and sixty-eight times of that at 30km, which results that near space propeller airfoils work at 10^4-10^5 Reynolds numbers. And the existence of the laminar separation bubble (LSB) on airfoils at 10^4-10^5 Reynolds numbers can reduce performances of low-Reynolds-number airfoils greatly.

Previous studies experimentally or numerically investigated characteristics of the LSB on airfoils at low Reynolds numbers. In 1967, The conventional time-averaged model of the LSB had been sketched by Horton using an semi-empirical theory [1]. In 1988, McGhee performed experiments for the E387 airfoil at low Reynolds numbers in the Langley Low-Turbulence Pressure Tunnel [2]. In 1996, Muti Lin studied the low-Reynolds-number separation on the E387 airfoil numerically [3]. In 2008, Jones investigated the behavior of the LSB formed on a NACA0012 airfoil by a combination of direct numerical simulation and linear stability analysis [4]. These researches showed that conventional airfoils had large separation regions and poor performances at low Reynolds numbers. Consequently, it is significantly necessary and meaningful to design the airfoil which behaves well at low Reynolds numbers, especially at 10^4-10^5 Reynolds numbers.

Received: June 8, 2015 Revised: June 15, 2015
Accepted: June 25, 2015
†Corresponding Author
Tel:+86-029-88491419
E-mail: zhangslnwpu@163.com

2. Numerical Setup

2.1. Numerical Methods

The governing equations (i.e. Navier-Stokes equations) in the integral form can be written as following [5]:

$$\iiint_{\Omega} \frac{\partial W}{\partial t} dV + \oiint_{\partial\Omega} \overline{\overline{H}} \bullet ndS = \oiint_{\partial\Omega} \overline{\overline{H_v}} \bullet ndS$$

where, Ω is the control volume. W is the flow variable vector, $\overline{\overline{H}}$ and $\overline{\overline{H_v}}$ denote inviscid flux vector and viscous flux vector respectively. These vectors are defined as following:

$$W = \begin{Bmatrix} \rho \\ \rho u \\ \rho v \\ \rho w \\ \rho E \end{Bmatrix}, \quad \overline{\overline{H}} = \begin{Bmatrix} \rho q \\ \rho uq + pI_x \\ \rho vq + pI_y \\ \rho wq + pI_z \\ \rho Hq \end{Bmatrix}, \quad \overline{\overline{H_v}} = \begin{Bmatrix} 0 \\ \tau_{xx}I_x + \tau_{xy}I_y + \tau_{xz}I_z \\ \tau_{xy}I_x + \tau_{yy}I_y + \tau_{yz}I_z \\ \tau_{xz}I_x + \tau_{yz}I_y + \tau_{zz}I_z \\ \beta_x I_x + \beta_y I_y + \beta_z I_z \end{Bmatrix}$$

where, $q = (u,v,w)^T$ is the velocity vector. I_x, I_y, I_z denote the unit vectors of Cartesian coordinates. ρ, p, E and H denote density, pressure, total en ergy per unit mass and total enthalpy per unit mass, respectively.

In addition, the finite-volume method with second-order spatial accuracy is used to solve the governing equations whilst the second-order accurate, implicit time-integration with dual time-stepping is utilized.

2.2. Computational Mesh

A "C-type" grid, sketched in Fig.1 and Fig.2, is employed in present airfoil computations. The computational domain extends from 20 chords upstream of the leading edge to 30 chords downstream of the tailing edge and 20 chords above and below the airfoil with one chord length in the spanwise direction. The grid contains 441 points wrapped over the airfoil and 125 points normal to the airfoil.

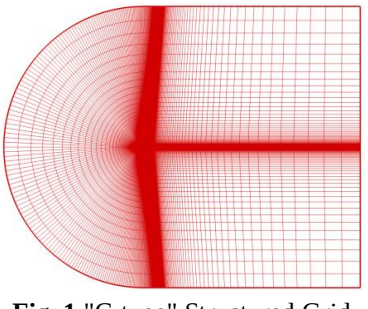

Fig. 1 "C-type" Structured Grid

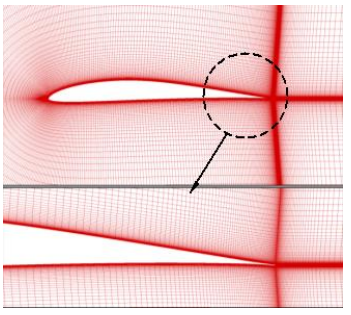

Fig. 2 Close-up View of the Grid for the E387 Airfoil

3. Results and Discussions

3.1. Method Validation

Firstly, E387 airfoil is studied at 0.05 Mach number (Ma), 6.0×10^4 Reynolds number (Re) and 4-deg angle of attack (AOA) to validate the numerical method. Table 1 shows the computed time-averaged lift coefficient (Cl), drag coefficient (Cd) and lift-to-drag ratio (L/D) which are compared with experimental results of McGhee [2]. Because of the existence of the LSB, 3.1% relative error of Cl, 4.0% relative error of Cd and no more than 1.0% relative error of L/D are tolerable.

Table 1 Numerical and Experimental Time-averaged Aerodynamics Coefficients of the E387 Airfoil (Ma=0.05, Re=6.0×10^4, AOA=4°)

	Cl	Cd	L/D
Numerical Results	0.663	0.0448	14.79
Experimental Results	0.643	0.0431	14.92
Relative Error	3.1%	4.0%	-0.9%

3.2. Analysis of the Novel Low-Reynolds-Number Airfoil

Considering that near space propeller airfoils work at 0-0.6 Mach number and small angle of attack besides at 10^4-10^5 Reynolds numbers, the low-Reynolds-number airfoil is designed typically at 0.3 Mach number, 5.0×10^4 Reynolds number and 3-deg angle of attack. Based on the airfoil which was raised by Srinath et al. using an adjoint method [6], the thickness and camber of the airfoil are further modified and optimized to achieve better performances by weakening the LSB. Finally, a novel low-Reynolds-number airfoil named SPLRM with the maximum thickness at about 85% chord, as shown in Fig.3, is designed. To evaluate the performance of the SPLRM airfoil and understand the LSB in depth,

another computation for the SD8040 airfoil at same conditions is conducted. Instantaneous streamlines and pressure contours of the SPLRM airfoil and SD8040 airfoil are shown in Fig.4 and Fig.5 for three equal time intervals respectively. Flows on both two airfoils are virtually unsteady while the generation, development and rupture of vortices can be observed. The separation occurs at about 70% chord on the suction side of SD8040 airfoil, which leads to the big separation bubble and large separation regions. But there is only small separation bubble and separation regions at the tail of the SPLRM airfoil.

Fig. 3 Novel Low-Reynolds-number Airfoil named SPLRM

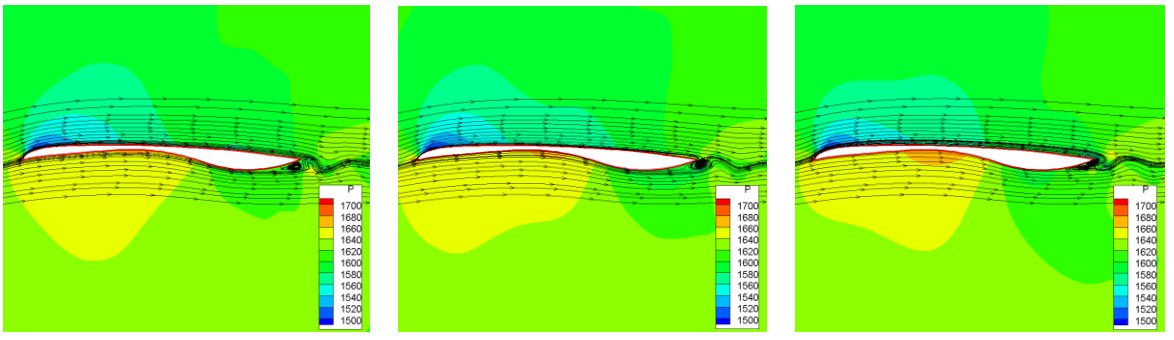

(a) t=T/3 (b) t=2T/3 (c) t=T

Fig. 4 Streamlines and Pressure Contours of the SPLRM Airfoil at Different Moments (T=period, Ma=0.3, Re=5.0×10^4, AOA=3°)

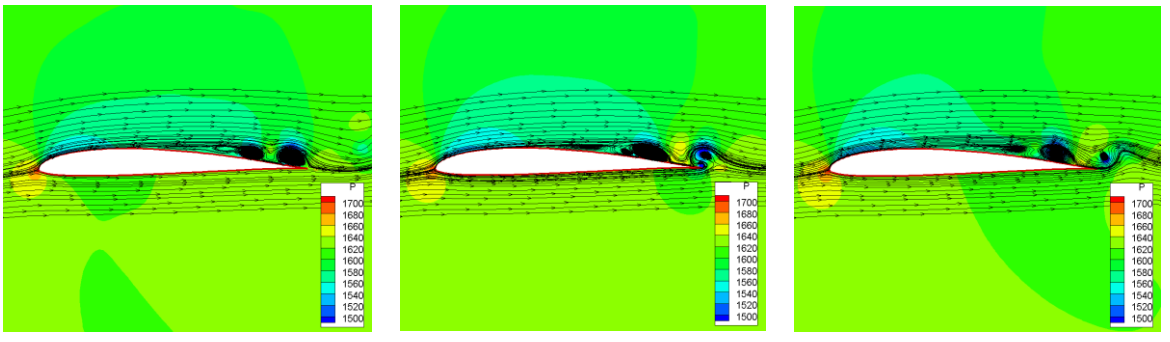

(a) t=T/3 (b) t=2T/3 (c) t=T

Fig. 5 Streamlines and Pressure Contours of the SD8040 Airfoil at Different Moments (T=period, Ma=0.3, Re=5.0×10^4, AOA=3°)

Table.2 summarizes time-averaged aerodynamic coefficients of the two airfoils. It can be seen that at the same AOA, Cl of the SPLRM airfoil is 21.7% higher than that of the SD8040 airfoil, and Cd of the SPLRM airfoil is 24.3% lower than that of the SD8040 airfoil. Similarly, at the almost same Cl by increasing the AOA of the SD8040 airfoil to 4.5 deg, Cd of the SPLRM airfoil is 51.4% lower than that of the SD8040 airfoil, thus L/D of the SPLRM airfoil is about 100% higher than that of the SD8040 airfoil.

Table 2 Time-averaged numerical results of SD8040 and SPLRM airfoils (Ma=0.3, Re=5.0×10^4)

Airfoils	AOA	Cl	Cd	L/D
SPLRM	3°	0.7120	0.03280	21.71
SD8040	3°	0.5850	0.04335	13.49
	4.5°	0.7289	0.06748	10.80

3.3. Reynolds Number Effect

To explore the Reynolds number effect, other computations are conducted at Reynolds numbers of 1.0×10^5, 1.5×10^5, 5.0×10^5 and 1.0×10^6 when Ma is 0.3 and AOA is 3°. When the Reynolds number is above 10^5, the SD8040 airfoil has higher lift-to-drag ratios than the SPLRM airfoil, as shown in Fig.6. This can be illustrated by Fig.7 and Fig.8. At the Reynolds number of above 10^5, the SD8040 airfoil has larger suction region and smaller separation region. However, as the Reynolds number increases, the high-pressure region of the SPLRM airfoil at the pressure side becomes smaller and smaller, and the

separation region at the tail keeps almost unchangeable. Thus, the SPLRM airfoil is more suitable for the Reynolds number of 10^4 -10^5.

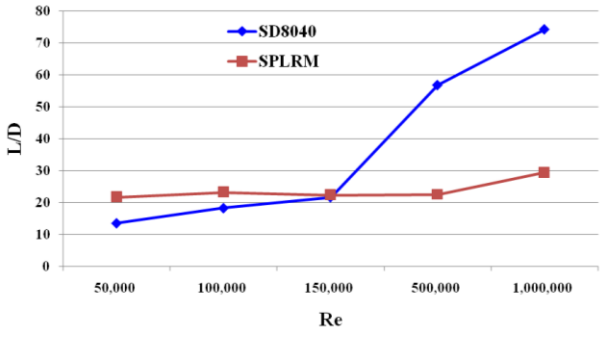

Fig. 6 Lift-to-drag Ratios of SD8040 and SPLRM airfoils at Different Reynolds Numbers(Ma=0.3, AOA=3°)

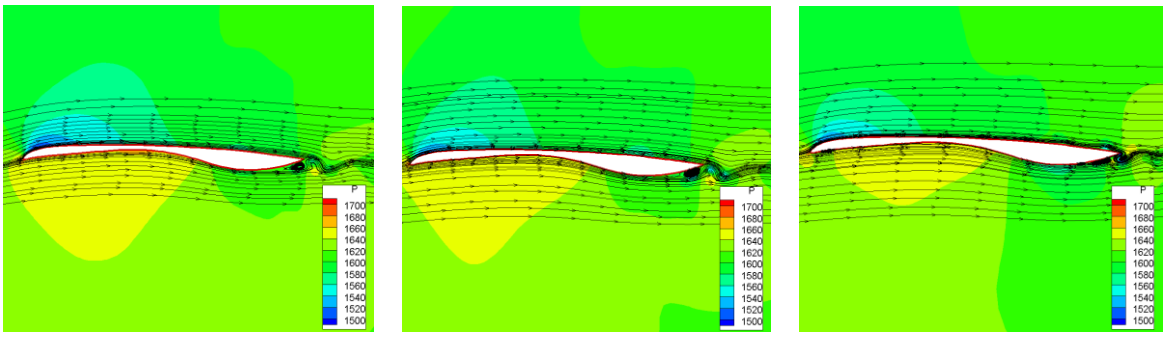

(a) Re=5.0×10^4 (b) Re=1.5×10^5 (c) Re=5.0×10^5

Fig. 7 Streamlines and pressure contours of the SPLRM airfoil at different Reynolds numbers (Ma=0.3, AOA=3°)

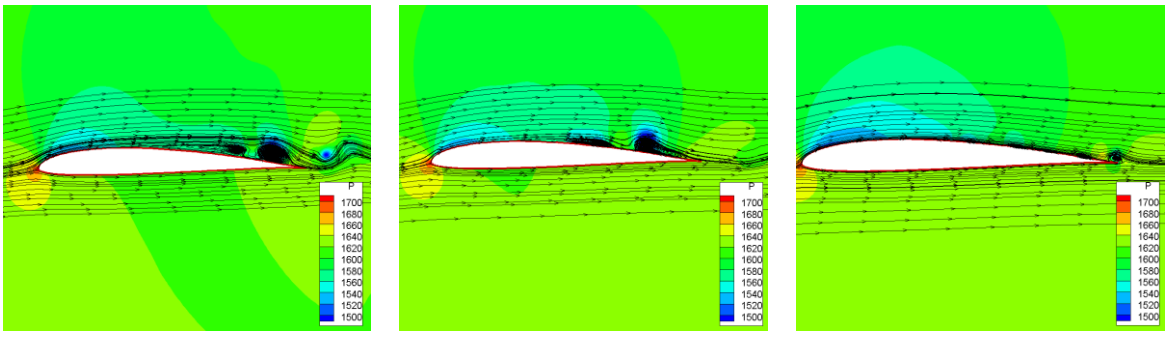

(a) Re=5.0×10^4 (b) Re=1.5×10^5 (c) Re=5.0×10^5

Fig. 8 Streamlines and pressure contours of the SD8040 airfoil at different Reynolds numbers (Ma=0.3, AOA=3°)

4. Conclusions

A novel low-Reynolds number airfoil named SPLRM is designed for near space propellers in this paper. Unsteady characteristics of the LSB on the SPLRM airfoil and SD8040 airfoil are studied, and the Reynolds number effect is investigated. Although the SD8040 airfoil behaves well when the Reynolds number is over 10^5, the larger high-pressure region and smaller separation region bring better performances for the SPLRM airfoil at 10^4-10^5 Reynolds numbers. For the fixed Reynolds number of 5.0×10^4, L/D of the SPLRM airfoil is about 100% higher than that of the SD8040 airfoil.

Acknowledgement

The research is funded by the National Natural Science Foundation of China (Grant No.11302177 & 11272263).

References

[1] H. P. Horton, "A Semi-Empirical Theory for the Grown and Bursting of Laminar Separation

Bubbles", *Aeronautical Research Council Current Papers*, CP 1073, 1967.

[2] R. J. McGhee, B. S. Walker and B. F. Millard, "Experimental results for the Eppler 387 airfoil at low Reynolds numbers in the langley low-turbulence pressure tunnel", *NASA*, TM4062, 1988.

[3] J. C. Muti Lin and L. L. Pauley, "Low-Reynolds-Number Separation on an Airfoil", *AIAA Journal*, vol.34, no. 8, pp. 1570-1576, 1996.

[4] L. E. Jones, "Numerical Studies of the Flow around an Airfoil at Low Reynolds Number", *Thesis for the degree of Doctor of Philosophy*, University of Southampton, 2008.

[5] J. R. Anderson, *Computational Fluid Dynamics - The Basics with Applications*, University of Maryland, 2002.

[6] D. N. Srinath and S. Mittal, "An adjoint method for shape optimization in unsteady viscous flows", *Journal of Computational Physics*, vol.229, pp. 1994-2008, 2010.

Authors

Shunlei Zhang

A PhD student at the school of aeronautics, Northwestern Polytechnical University in Xi'an, China.

He majors in Aircraft Design Engineering and Fluid Mechanics. Now he focuses on the design of low-Reynolds-number airfoils and propellers.